Semiconductor Physics, Quantum Electronics & Optoelectronics, 2009. V. 12, N 4. P. 391-398.

PACS 87.64.-t

Wavelet analysis for Mueller matrix images of biological crystal networks

Yu.O. Ushenko, Yu.Ya. Tomka, O.G. Pridiy, A.V. Motrich, O.V. Dubolazov, I.Z. Misevitch, V.V. Istratiy
Chernivtsi National University, Optics and Spectroscopy Dept., Chernivtsi, Ukraine, 58000

Abstract. Theoretically grounded in this work is the efficiency of using the statistical and fractal analyses for distributions of wavelet coefficients for Mueller-matrix images of biological crystal networks inherent to human tissues. The authors found interrelations between statistical moments and power spectra for distributions of wavelet coefficients as well as orientation-phase changes in networks of biological crystals. Also determined are criteria for statistical and fractal diagnostics of changes in the birefringent structure of biological crystal network, which corresponds to pathological changes in tissues.

Keywords: polarization, Mueller matrix, biological crystal, birefringence, statistical moment, wavelet analysis, fractal.

Manuscript received 28.05.09; accepted for publication 10.09.09; published online 30.10.09.

1. Introduction

In recent years, laser diagnostics aimed at the structure of biological tissues efficiently uses the model approach [1], in accord with which the tissues are considered as two components: amorphous $\{A\}$ and optically anisotropic $\{M\}$ ones. Topicality of this modeling is related with the possibility to apply the all-purpose Mueller matrix analysis to changes of polarization properties, which are caused by transformation of optical-and-geometric constitution of the anisotropic component (architectonic network of fibrils) in these biological objects [2 – 8]. Based on this model, there developed is the method for polarization differentiation of optical properties inherent to physiologically normal as well as pathologically changed biological tissues by using the wavelet analysis of local features observed in coordinate distributions of intensities in their coherent images.

This trend in polarization diagnostics got its development in investigations of a statistical and self-similar structure of Mueller-matrix images (MMI) that are two-dimensional distributions $f_{ik}(x,y)$ [9,10] describing biological tissues. So, in the approximation of single light scattering, there found was the interrelation between a set of statistical moments of the first to fourth orders $Z^{(j=1,2,3,4)}$ that characterize orientation (ρ) and phase (δ) structures of birefringent architectonics inherent to biological tissues as well as a set of respective statistical moments for MMI [10 – 14]. It is ascertained that the coordinate distributions of matrix elements $f_{ik}(x,y)$ describing physiologically normal biological tissue possess a self-similar, fractal structure. While MMI of physiologically changed biological tissues are stochastic or statistical [11].

This work is aimed at studying the efficiency of the wavelet analysis in application to the local structure of MMI inherent to biological tissues with using statistical and fractal analyses of the obtained wavelet-coefficient distributions for diagnostics of local changes in orientation-phase structure of their architectonic networks.

2. Wavelet analysis of Mueller-matrix images of biological tissues

Wavelet transformation of MMI consisted of its expansion within a basis of definite scale changes and transfers of the soliton-like function (wavelet) [5]. The distribution of values for f_{ik} elements of the Mueller matrix can be represented in the following form:

$$f_{ik}(x) = \sum_{j,l=-\infty}^{\infty} q_{jl} \upsilon_{jl}(x). \qquad (1)$$

Here, $f_{ik}(x)$ distribution belongs to the space $L^2(R)$ created by wavelets υ_{jl}. The basis of this functional space can be constructed using scale transformations and transfers of the wavelet $\upsilon_{jl}(x)$ with arbitrary values of basic parameters – the scaling coefficient a and shift parameter b

$$\upsilon_{ab}(x)=\left|a^{-1/2}\right|\xi\left(\frac{x-b}{a}\right);a,b\in R;\xi\in L^2(R). \qquad (2)$$

Being based on it, the integral wavelet transformation takes a look

$$[W_\upsilon f_{ik}](a,b)=|a|^{-1/2}\int_{-\infty}^{\infty}f_{ik}(x)\upsilon^*\left(\frac{x-b}{a}\right)dx=$$
$$=\int_{-\infty}^{\infty}f_{ik}(x)\upsilon_{ab}{}^*(x)dx. \qquad (3)$$

Coefficients $q_{jl}=\langle f_{ik},\upsilon_{jl}\rangle$ of the expansion (3) for the function f_{ik} by wavelets can be defined via the following integral wavelet transformation

$$q_{jl}=[W_\upsilon f_{ik}]\left(\frac{1}{2^j},\frac{l}{2^j}\right). \qquad (4)$$

In our work, to analyze MMI we used the most widely spread soliton-like function MHAT ("Mexican hat", [5]) as a wavelet function.

3. Computer modeling the efficiency of the wavelet analysis to differentiate MMI of birefringent fibrils

Birefringent architectonic networks of BT consist of a set of co-axial cylinder protein fibrils with a statistical distribution of optical axis orientations ρ and values of phase shifts δ. We considered the most spread case of pathological changes in BT architectonics – formation of directions for pathological growth or excrescence of a tumor. Within mathematical frames, this case was modeled as a superposition of statistical (equiprobable) and stochastic (quasi-regular) components in distributions of orientations ρ of birefringent fibrils as well as phase shifts δ that are caused by them

$$\begin{cases}Q_1(\rho)\approx R(\rho)+A\sin\dfrac{2\pi}{D}\rho,\\ Q_2(\delta)\approx R(\delta)+B\sin\dfrac{2\pi}{D}\delta.\end{cases} \qquad (5)$$

where $Q_{i=1,2}$ are the functions of distributions for ρ and δ values; R – random (equiprobable) distribution of ρ and δ; A, B – amplitudes of the stochastic component; D – mean statistical size of co-axial fibrils.

In accord with distributions of optical-and-geometrical parameters $Q_i(\rho,\delta)$, the distribution of values for Mueller matrix elements f_{ik} for such a territorial matrix can be written in the form

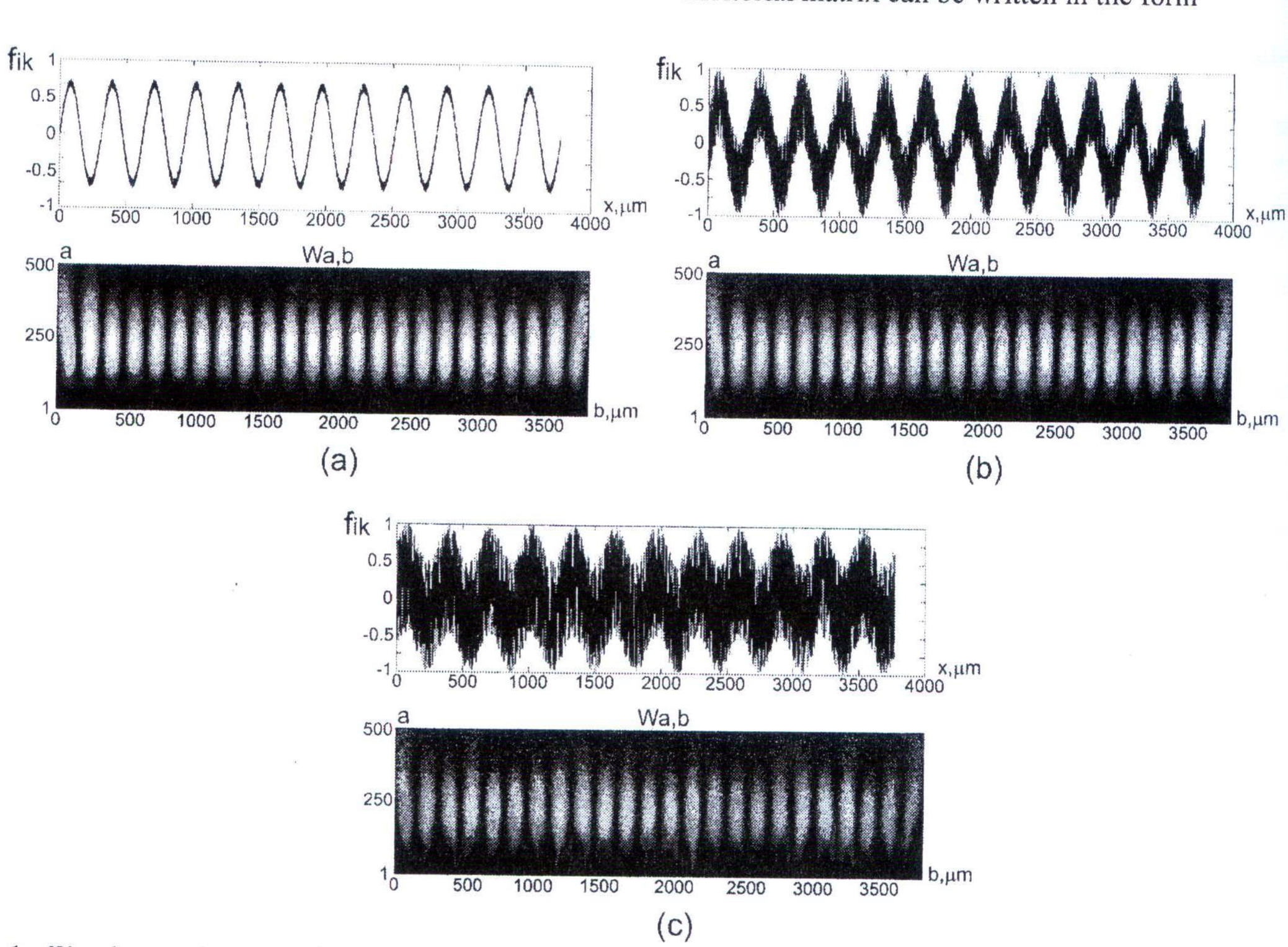

Fig. 1. Wavelet coefficients $W_{a,b}$ of statistical-and-stochastic distributions for the matrix element $f_{ik}(b)$ (a, b, c). Commentaries are in the text.

$$f_{ik}(\rho,\delta) = R(\rho,\delta) + C\sin\frac{2\pi}{D} f_{ik}(\rho,\delta)\,. \qquad (6)$$

Here, C is the amplitude of a stochastic component. We modeled a superposition of a "background" $R(\rho,\delta)$ and informative signal $C\sin\frac{2\pi}{D}F_{ik}(\rho,\delta)$ for the following relations between their amplitudes $R(\rho,\delta) = 0.01\cdot C\sin\frac{2\pi}{D} f_{ik}(\rho,\delta) \div 6\cdot C\sin\frac{2\pi}{D} f_{ik}(\rho,\delta)$.

Fig. 1 shows wavelet coefficients $W_{a,b}$ for the respective distributions $f_{ik}(\rho,\delta)$.

As seen from the data obtained, the distributions of values for wavelet coefficients $W_{a,b}$ of all the types of signals $f_{ik}(\rho,\delta)$ behave like quasi-harmonic structures. Even in the case of significant (six-fold) dominance of the statistical component amplitude (Fig. 1, c), the quasi-regular structure of coordinate distribution for wavelet coefficients $W_{a,b}$ is preserved in full. This fact confirms a high efficiency of the wavelet analysis in separation of the harmonic component in the distribution of f_{ik} elements of the Mueller matrix.

To make diagnostic possibilities of the wavelet analysis more objective, we calculated statistical moments of the first to fourth orders (M, σ, A, E), which characterize distributions of the wavelet coefficients $W_{a,b}(f_{ik})$ for various ratios $0.01 \le \frac{A_0}{A} \le 6$ (Fig. 2) and found their power spectra (Table 1).

Our analysis of the obtained data revealed that the change of the fourth statistical moment for the distribution of wavelet coefficients $W_{a,b}$ is the most dynamical from the above viewpoint, as the value of this moment changes within the range of one order in dependency of ratios $0.01 \le \frac{A_0}{A} \le 6$.

Our investigation of log-log dependences for power spectra of distributions describing the wavelet coefficients $W_{a,b}$ of matrix elements f_{ik} allowed revealing the following regularities:

- all the dependences $\log W_{a,b} - \log(1/d)$ calculated for various relations between amplitudes of random and quasi-regular components of distributions characteristic for the Mueller matrix elements f_{ik} consist of two parts, namely: the fractal one (with one slope of the approximating curve within a definite range Δd for sizes of birefringent fibrils) and the statistical one (when a stable value for the slope angle of the approximating curve does not take place);

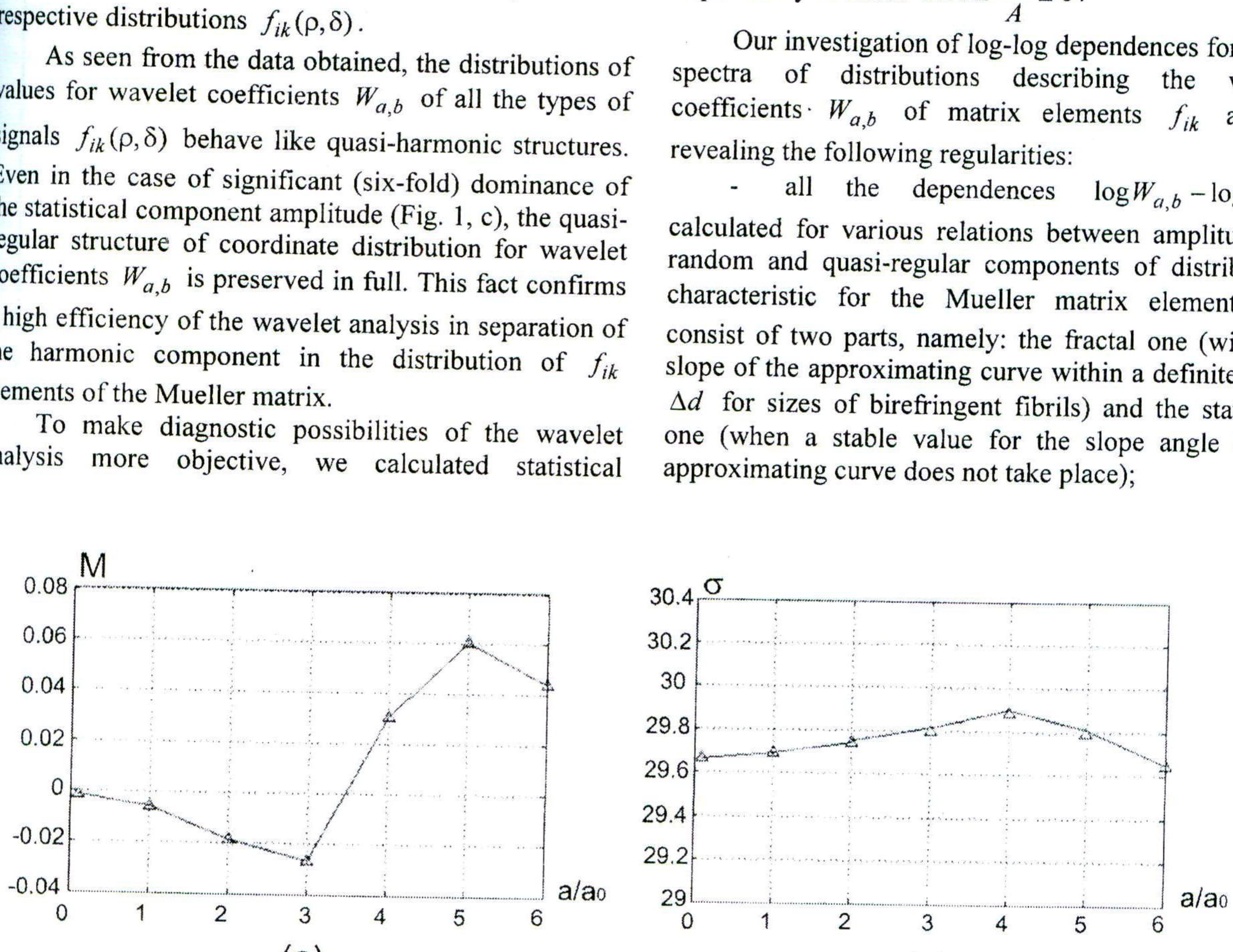

Fig. 2. Mean value (a), dispersion (b), asymmetry (c) and excess (d) of distributions inherent to wavelet coefficients $W_{a,b}(f_{ik})$. Commentaries are in the text.

- when the amplitude of the statistical component in the f_{ik} distribution grows, the range Δd of a linear part in dependences $\log W_{a,b} - \log(1/d)$ is decreased;

- fractal component of log-log dependences for the power spectra of wavelet coefficients $W_{a,b}$ is preserved even for significant (six-fold) dominance of the noise amplitude and comprises the size range $\Delta d = 50 - 100$ μm.

Thus, the performed computer modeling indicates the diagnostic efficiency of the wavelet analysis when detecting local changes in birefringency (δ) of ordered biological crystals.

Table 1. Log-log dependences of power spectra for the wavelet coefficients $W_{a,b}$ of statistical-stochastic distributions for f_{ik} elements of the Mueller matrix describing single-axis biological crystals

ΔR	$\log W_{a,b} - \log(1/d)$	$\Delta d, \mu m$	ΔR	$\log W_{a,b} - \log(1/d)$	$\Delta d, \mu m$
0.01	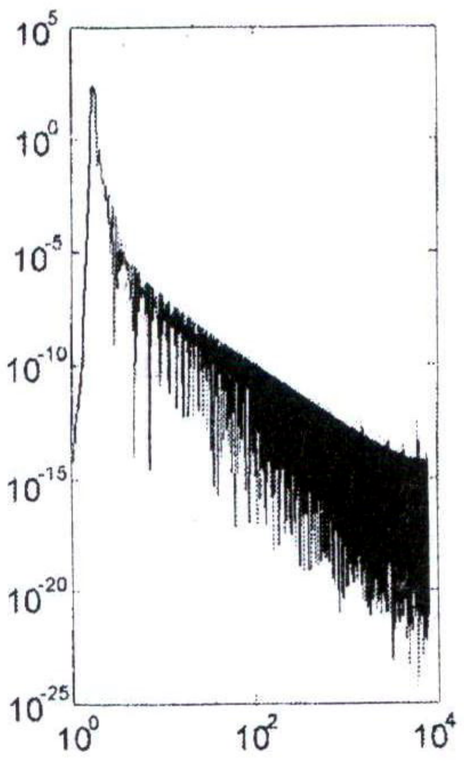	*1-1000*	1	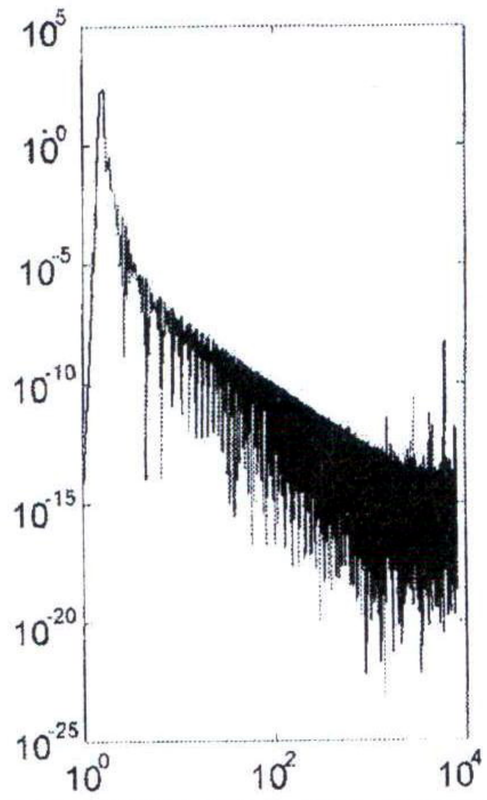	*5-100*
0.1	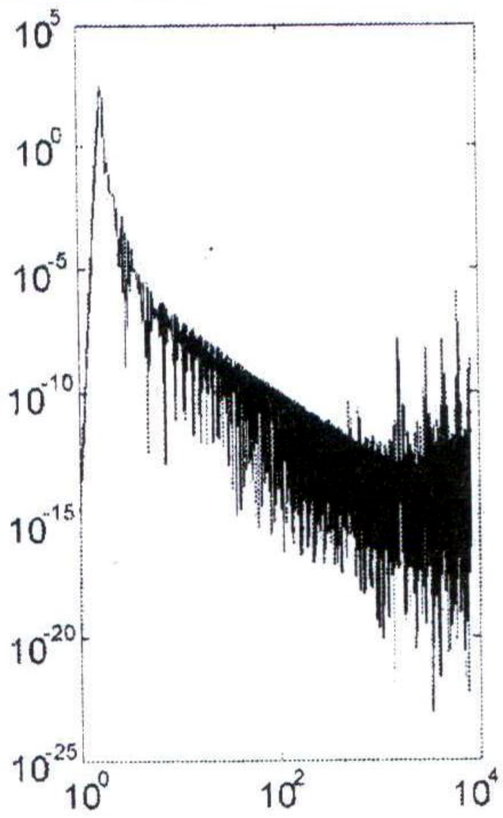	*5-1000*	3	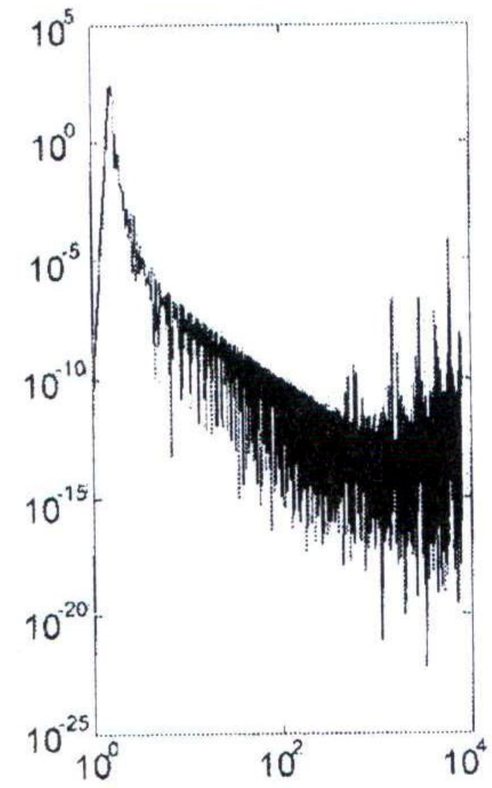	*20-100*
0.5	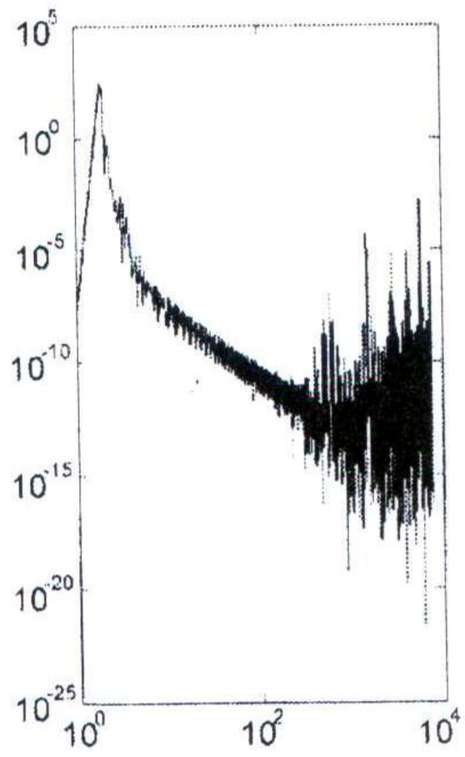	*5-100*	6	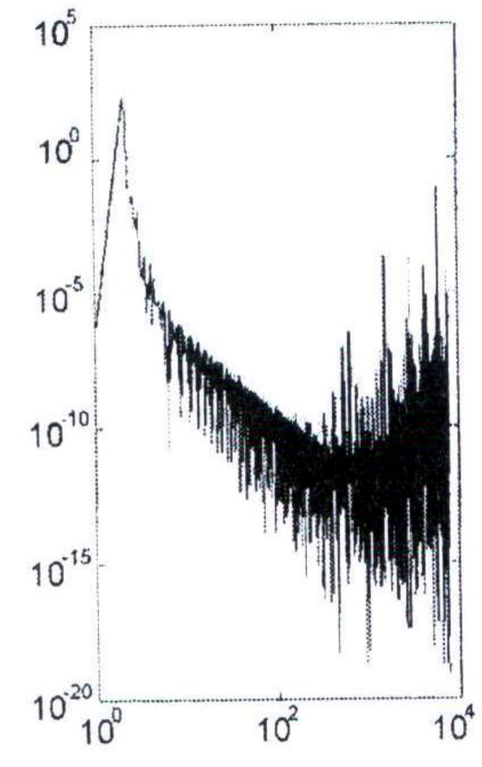	*50-100*

Besides, using the statistical and correlation analysis of wavelet coefficients $W_{a,b}$ in the expansion of the Mueller matrix elements, we have demonstrated the possibility to reveal the quasi-harmonic component in distributions of orientation (ρ) and phase (δ) parameters in complex (statistical) architectonic networks.

4. Diagnostics of local changes in the optical-and-geometrical structure of architectonic networks inherent to real biological tissues

We performed comparative investigations of two types of mounts from connective tissue of a woman matrix:

- healthy tissue (type A) – the set of chaotically oriented collagen fibrils;
- tissue in the state of displasia (pre-cancer state – type B) – the set of chaotically oriented collagen fibrils with local quasi-ordered parts.

From the optical viewpoint, polarization properties of these tissues (types A and B) are similar to some extent. For instance, the coordinate distribution of random values inherent to phase shifts $\delta(x, y)$, which is related with the range of changes in geometric sizes of collagen fibrils, is close in both cases. The main differences in composition of the set of biological crystals lie in presence of local parts with quasi-ordered directions of optical axes in the tissue of the type B. Being based on this fact, one can assume that the coordinate distribution of the Mueller matrix element values for the type A tissue $f_{ik}(\rho,\delta)$ approaches to the statistical one. The coordinate distribution $f_{ik}(\rho,\delta)$ for the type B tissue can be represented by a superposition of the random $R_{ik}(\rho,\delta)$ and quasi-regular $C\sin\frac{2\pi}{D}f_{ik}(\rho,\delta)$ components (6).

As a main element of the Mueller matrix for bio-tissue of a given type, we chose the "orientation" matrix element f_{33}. It is known that the statistical and correlation analysis of coordinate distributions for this element is considered as efficient in differentiation of

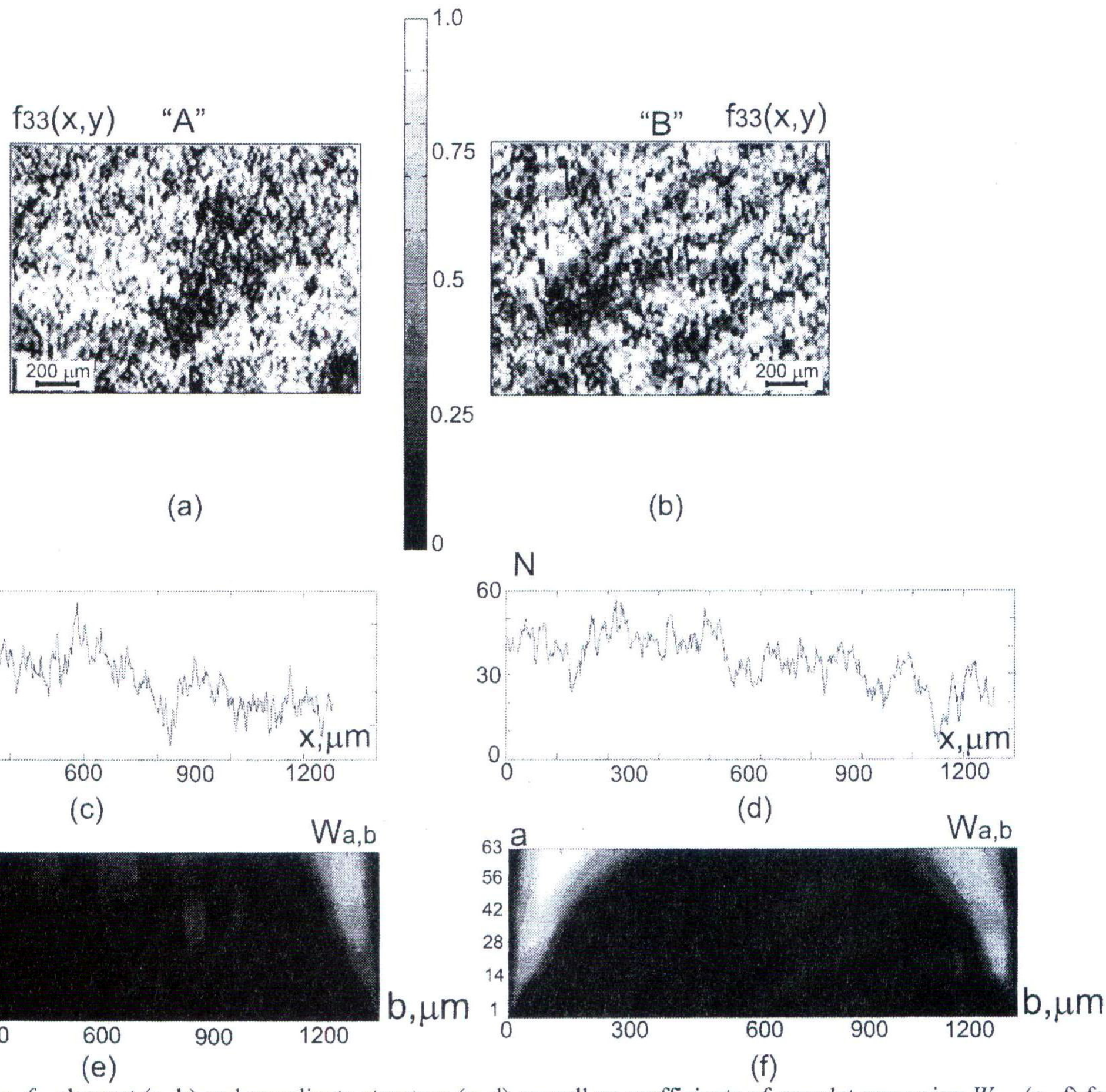

Fig. 3. MMI of the f_{33} element (a, b) and coordinate structure (c, d) as well as coefficients of wavelet expansion $W_{a,b}$ (e, f) for the f_{33} element of A and B type connective tissues.

optical properties characterizing collagen networks in healthy and pathologically changed skin [12].

Shown in Fig. 3 are MMI for the element f_{33} (fragment a – type A, fragment b – type B) and respective wavelet expansions (fragments e and f for the linear cross-section of $f_{33}(x, y)$, fragments c and d for healthy and pathologically changed connective tissue of the uterus neck.

Our comparative analysis of the obtained data shows a complex statistical structure of two-dimensional distributions for the matrix element $f_{33}(x, y)$ (see fragments a and b) as well as its linear cross-sections (fragments c and d) for MMI of bio-tissues for their both types.

The same can be stated for the distributions of wavelet coefficients $W_{a,\,b}$ (fragments e and f).

With account of the above observations, it seems actual to verify the efficiency of statistical (the set of the first to fourth moments for $W_{a,\,b}$ distributions) and correlation (features of the power spectra for wavelet coefficients of $W_{a,\,b}$) methods of analysis for diagnostics of formation of local parts containing quasi-ordered ($\rho(x, y) \approx$ const) birefringent fibrils.

Table 2. Log-log dependences of power spectra for the wavelet coefficients $W_{a,\,b}$ of statistical-stochastic distributions for the f_{33} element of A and B type connective tissues

a	"A"	"B"
14	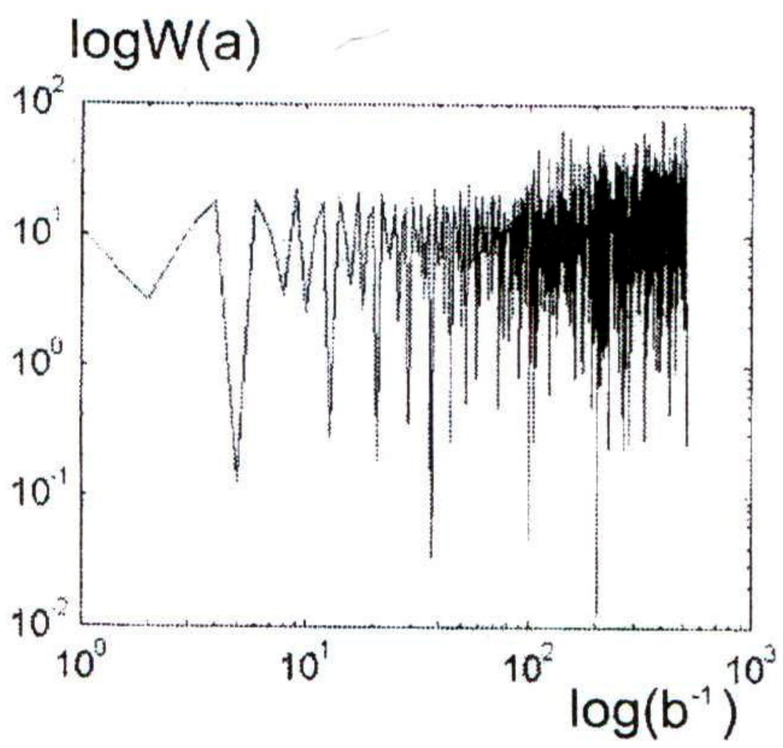	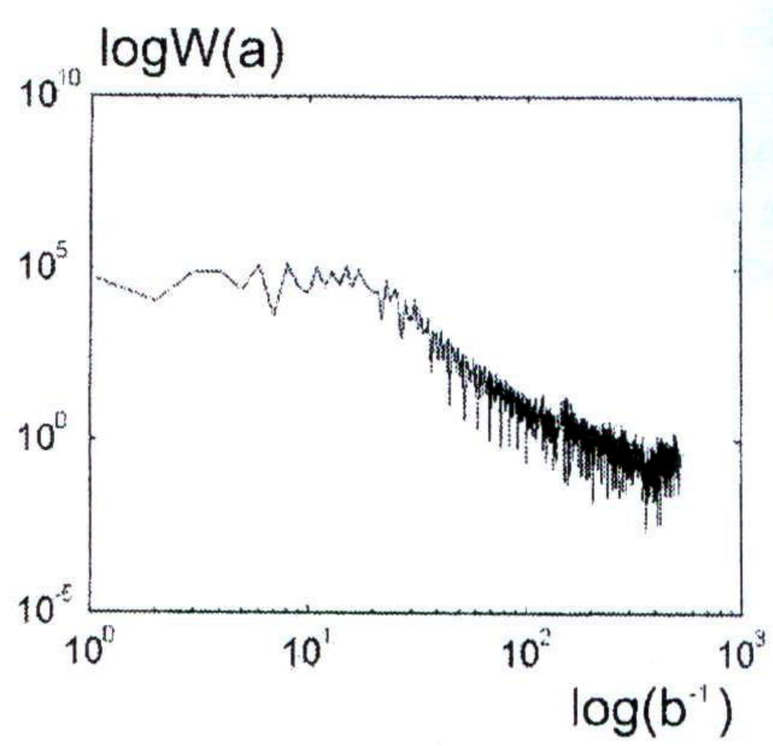
42	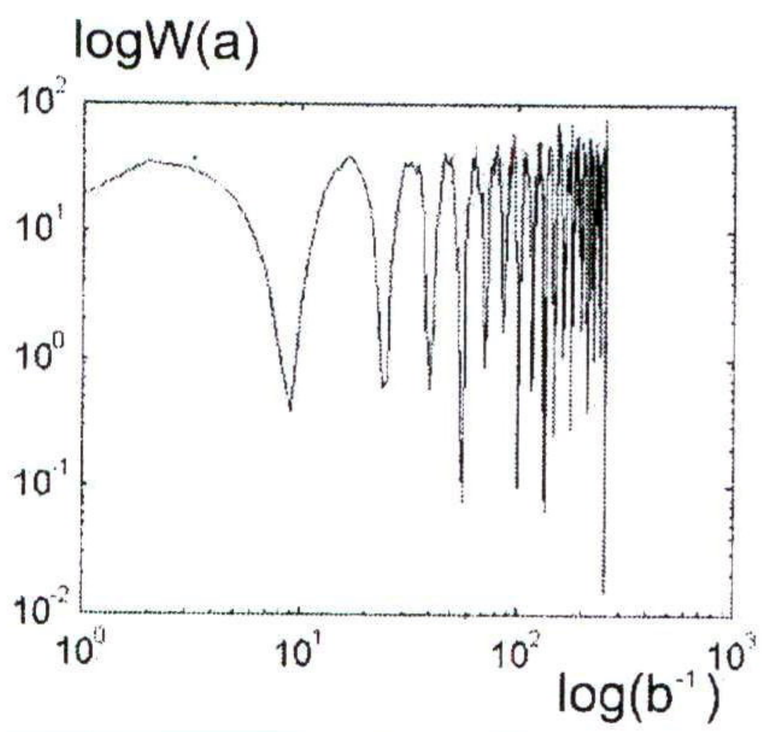	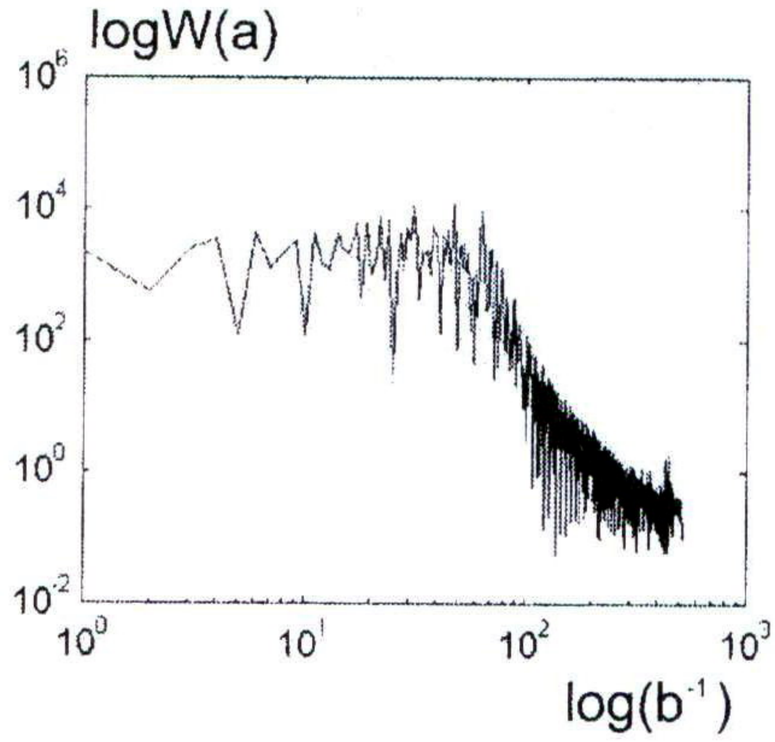
70	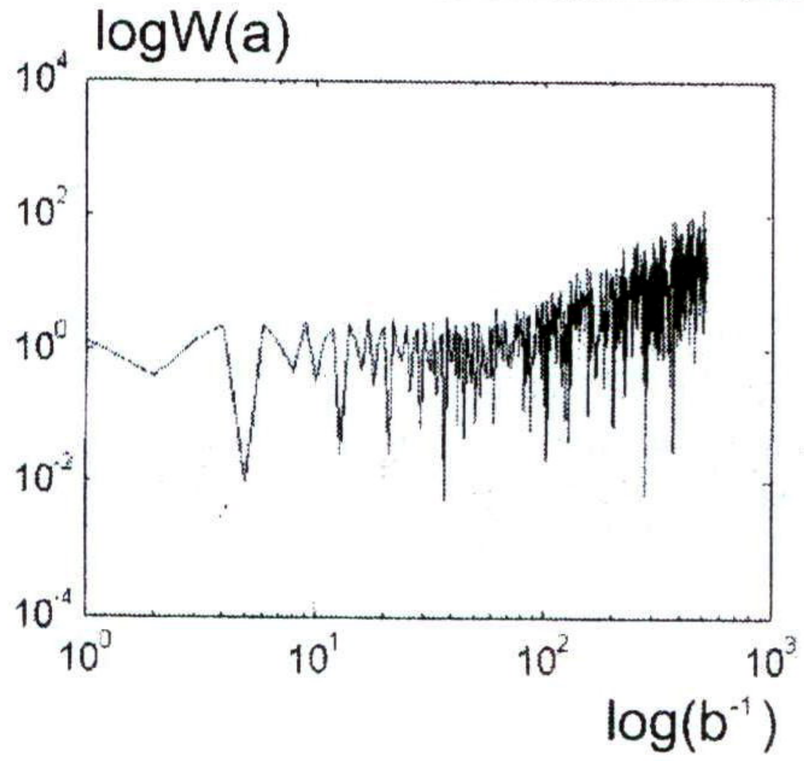	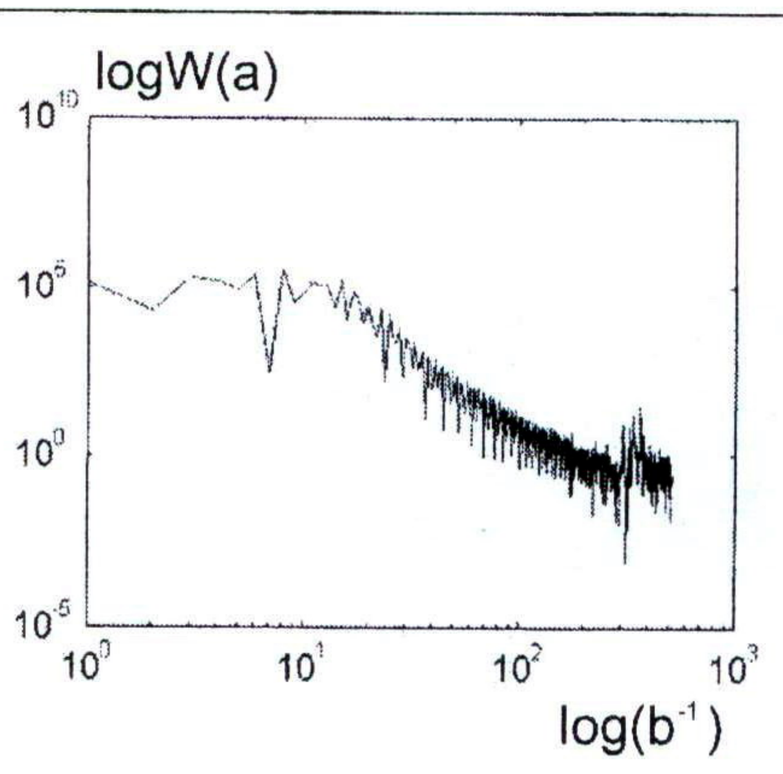

With this aim, we performed step-by-step "screening" the pictures for wavelet coefficients $W_{a,b}$ (Fig. 3, *e* and *f*) using the scale change for the wavelet function $\mu = 0.5$. For each value of the wavelet function a_i, we found the dependences $W(b, a = a_i)$ and calculated the log-log dependences for the scale of their power spectra. As a result of this linear scanning, we obtained the array of data $\{\log W(a_1) - \log(b)\} \div \{\log W(a_j) - \log(b)\}$ summarized in Table 2.

Coordinate distributions for the matrix element f_{33} corresponding to a mount of the sample of healthy connective tissue (Table 2) are characterized by statistical distributions for the wavelet coefficients $W_{a,b}$ in all the range of scale a changes of the wavelet function μ. It is confirmed by the absence of any stable slope of the approximating curve for the considered set of dependences $\log W_{a,b}(1 \le a \le 5b) - \log(b^{-1})$.

Another picture can be observed for the sample of changed connective tissue (Fig. 3). If the scale coefficient a of the wavelet function μ possesses some definite dimension, then there exist a linear part in the respective log-log dependence of the power spectrum characterizing the distribution of wavelet coefficients $W_{a,b}(a_i)$. In accord with performed computer modeling, this fact indicates the availability of a quasi-harmonic component in $W_{a,b}(a_i)$ distributions, which is caused by respective geometry of biological crystals.

In our case, for the mean statistical size of a pathological creation $a = 28$ μm one can observe a quasi-ordered part of collagen fibrils with sizes lying within the range 10 to 50 μm.

Thus, one can state that the correlation approach in the analysis of $W_{a,b}$ coefficients valid for the wavelet distribution in MMI of "orientation" element f_{33} for connective tissue of the uterus neck is rather efficient for differentiation of its healthy and pathologically changed samples.

Some additional information for differentiation of these objects was obtained using the statistical analysis of coordinate distributions $W_{a,b}(a_i)$.

Shown in Fig. 4 are the dependences of statistical moments of the 1st to 4th orders for coordinate distributions of wavelet coefficients $W_{a,b}$ in MMI of f_{33}, which corresponds to different scales of the wavelet function μ.

The obtained data show:

- statistical moments of the 1st and 4th orders for distributions of wavelet coefficients $W_{a,b}$, like to the case of computer modeling (Fig. 2) the f_{33} element describing the samples of connective tissues of both types, suffer insignificant changes (0 to 0.2) within the

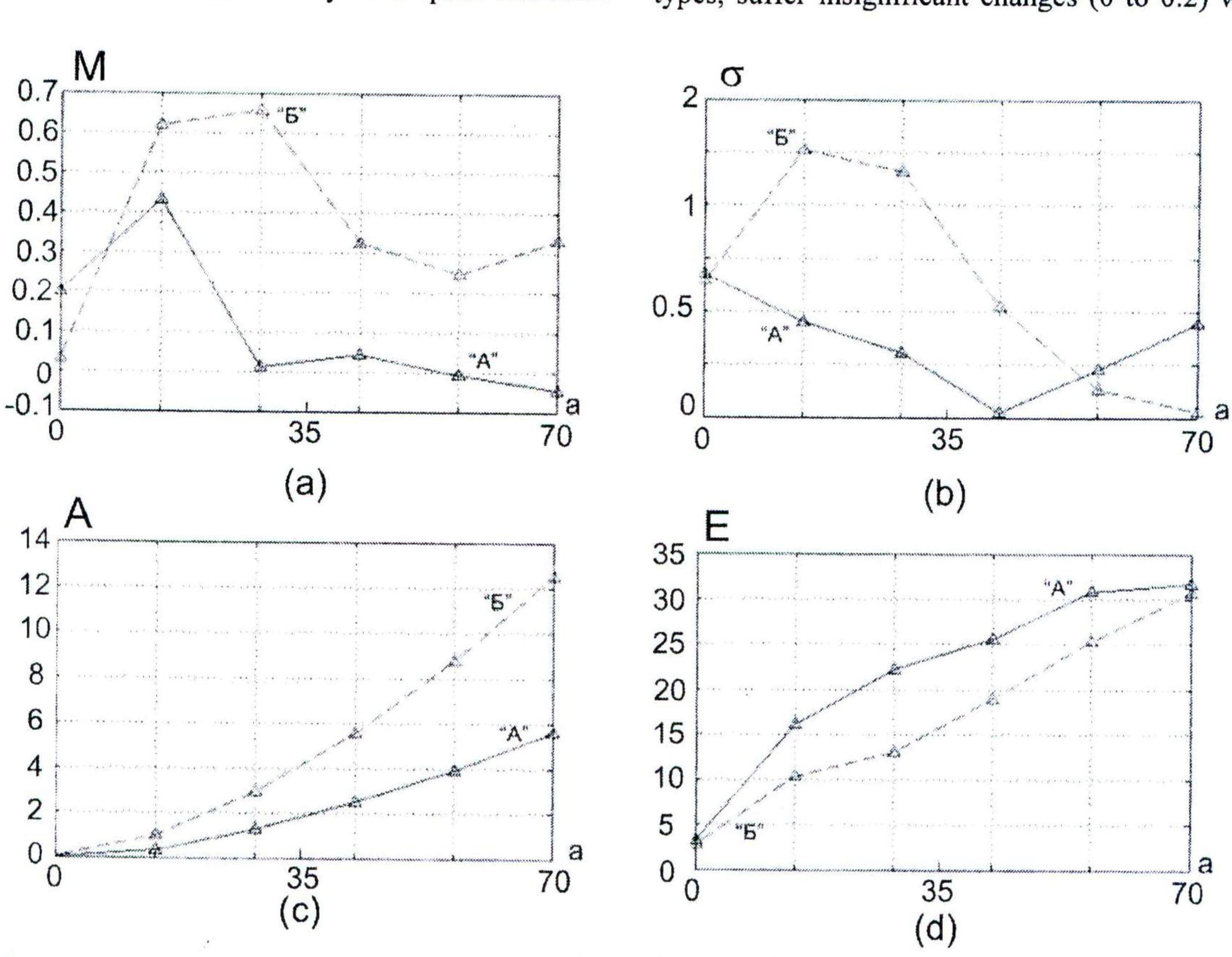

Fig. 4. Dependences of statistical moments of the 1st (a), 2nd (b), 3rd (c) and 4th (d) orders on the scale of the wavelet function μ for connective tissue of A and B types.

whole range of scales a_i for the wavelet function μ (Fig. 4);

- the range of changes in values of asymmetry (A) and excess (E) for $W_{a,b}$ distributions lie within the range of two orders (Fig. 4);

- main differences between connective tissues of A and B types are found in the vicinity of the scale $a = 28$ μm where dependences between $A(a)$ and $E(a)$ reach two- or three-fold level.

Thus, we found that the differences between values of statistical moments of higher orders for a definite range of scales a of the wavelet function μ_a can be also used to differentiate local changes in orientation changes of optical axes inherent to territorial matrix crystals.

References

1. S.C. Cowin, How is a tissue built? // *J. Biomed. Eng.* **122**, p. 553-568 (2000).
2. O.V. Angelsky, A.G. Ushenko, Yu.A. Ushenko, Ye.G. Ushenko, Yu.Ya. Tomka, V.P. Pishak, Polarization-correlation mapping of biological tissue coherent images // *J. Biomed. Opt.* **10**, No. 6, 064025 (2005).
3. J.F. de Boer and T.E. Milner, Review of polarization sensitive optical coherence tomography and Stokes vector determination // *J. Biomed. Opt.* 7, p. 359-371 (2002).
4. J.F. de Boer, T.E. Milner and J.S. Nelson, Two dimensional birefringence imaging in biological tissue using phase and polarization sensitive optical coherence tomography // In: *Trends in Optics and Photonics (TOPS): Advances in Optical Imaging and Photon Migration.* OSA, Washington, DC, 1998.
5. M.J. Everett, K. Shoenenberger, B.W. Colston and L.B. Da Silva, Birefringence characterization of biological tissue by use of optical coherence tomography // *Opt. Lett.* **23**, p. 228-230 (1998).
6. A.G. Ushenko, D.N. Burkovets, Wavelet-analysis of two-dimensional birefringence images of architectonics in biotissues for the diagnostics of pathological changes// *J. Biomed. Opt.* **9**, No. 4, p. 1023-1028 (2004).
7. O.V. Angelsky, Yu.Y. Tomka, A.G. Ushenko, Ye.G. Ushenko, S.B. Yermolenko, Yu.A. Ushenko, 2-D tomography of biotissue images in pre-clinic diagnostics of their pre-cancer states // *Proc. SPIE* **5972**, p. 158-162 (2005).
8. O.V. Angelsky, A.G. Ushenko, D.N. Burcovets, Yu.A. Ushenko, Polarization visualization and selection of biotissue image two-layer scattering medium // *J. Biomed. Opt.* **10**, No. 1, 014010 (2005).
9. O.V. Angelsky, Yu.Ya. Tomka, A.G. Ushenko, Ye.G. Ushenko and Yu.A. Ushenko, Investigation of 2D Mueller matrix structure of biological tissues for pre-clinical diagnostics of their pathological states // *J. Phys. D: Appl. Phys.* **38**, p. 4227-4235 (2005).
10. Shuliang Jiao, Wurong Yu, George Stoica, Lihong V. Wang. Optical-fiber-based Mueller optical coherence tomography // *Opt. Lett.* **28**, p. 1206-1208 (2003).
11. Yu.A. Ushenko, Statistical structure of polarization-inhomogeneous images of biotissues with different morphological structures // *Ukrainian Journal of Physical Optics* **6**, No. 2, p. 63-70 (2005).
12. O.V. Angelsky, A.G. Ushenko, Yu.A. Ushenko, Ye.G. Ushenko, Yu.Ya. Tomka, V.P. Pishak, Polarization-correlation mapping of biological tissue coherent images // *J. Biomed. Opt.* **10**, No. 6, 064025 (2005).
13. O.V. Angelsky, A.G. Ushenko, and Yu.A. Ushenko, Polarization reconstruction of orientation structure of biological tissues birefringent architectonic nets by using their Mueller-matrix speckle-images // *J. Holography Speckle* **2**, p. 72-79 (2005).
14. A.G. Ushenko, and V.P. Pishak, Laser Polarimetry of Biological Tissue. Principles and Applications, In: *Coherent-Domain Optical Methods. Biomedical Diagnostics, Environmental and Material Science (V.Tuchin, ed.).* Kluwer Academic Publishers, 2004, p. 67-93.